Delft University of Technology

Document Version
Final published version

Licence
CC BY-NC

Citation (APA)
Doong, D. J., Lee, Y. C., Tseng, L. H., & Chen, Y. C. (2026). A site-specific classification of typhoon-induced coastal hazards based on compound extreme waves and storm surges. *Journal of Sea Research*, *214*, Article 102736. https://doi.org/10.1016/j.seares.2026.102736

Important note
To cite this publication, please use the final published version (if applicable).
Please check the document version above.

Copyright
In case the licence states “Dutch Copyright Act (Article 25fa)”, this publication was made available Green Open Access via the TU Delft Institutional Repository pursuant to Dutch Copyright Act (Article 25fa, the Taverne amendment). This provision does not affect copyright ownership.
Unless copyright is transferred by contract or statute, it remains with the copyright holder.

Sharing and reuse
Other than for strictly personal use, it is not permitted to download, forward or distribute the text or part of it, without the consent of the author(s) and/or copyright holder(s), unless the work is under an open content license such as Creative Commons.

Takedown policy
Please contact us and provide details if you believe this document breaches copyrights.
We will remove access to the work immediately and investigate your claim.

This work is downloaded from Delft University of Technology.

Journal of Sea Research 214 (2026) 102736

Contents lists available at ScienceDirect

Journal of Sea Research

journal homepage: www.elsevier.com/locate/seares

A site-specific classification of typhoon-induced coastal hazards based on compound extreme waves and storm surges

Dong-Jiing Doong [a,b], Yu-Chen Lee [b,c,*], Leng-Hsuan Tseng [d], Ying-Chih Chen [b]

[a] Department of Hydraulic and Ocean Engineering, National Cheng Kung University, Tainan, Taiwan
[b] Coastal Ocean Monitoring Center, National Cheng Kung University, Tainan, Taiwan
[c] Delft Center for Systems and Control, Mechanical Engineering, Delft University of Technology, Delft, the Netherlands
[d] Environmental Engineering and Water Technology Department, Institute for Water Education, Delft, the Netherlands

ARTICLE INFO

Keywords:
Joint probability
Typhoon
Storm surge
Compound extreme value distribution
Copula
Typhoon-induced coastal hazard classification

ABSTRACT

Accurate estimation of coastal hazards requires considering the dependence between extreme wave heights and storm surges particularly in regions affected by typhoons. This study analyzes the joint probability of these variables using approximately 14 years of field observations from Taiwan. An event-based sampling method was adopted, utilizing a new definition of the typhoon influence period to isolate extreme events. The dependence structure was modeled using bivariate copulas with the Gumbel–Hougaard (GH) copula and Generalized Extreme Value (GEV) marginal distributions. These were integrated with a Poisson model to form a Compound Extreme Value Distribution (CEVD). The results indicate that design values derived from joint return periods provide a more realistic assessment of risk compared to univariate methods. Furthermore, a new typhoon-induced coastal hazard classification scheme based on these joint probabilities is proposed, providing a more effective tool for coastal hazard warning and assessment.

1. Introduction

Coastal hazards induced by extreme systems are not determined by a single factor (Igigabel et al., 2023). Large waves endanger coastal safety by causing the failure of coastal infrastructures and inundating coastal regions. They may also threaten the lives of people living at the shoreline (Cuomo et al., 2011; Li et al., 2008; Salvadori et al., 2014). High water levels combined with high storm surges also cause damage, such as coastal flooding, erosion, dike overtopping, as well as changes to the coastal ecosystem (Corbella and Stretch, 2012; Li et al., 2013; Islam et al., 2019). When these extreme events occur simultaneously, they can generate the maximum potential damage to coastal infrastructure and communities. Compound coastal hazards are not limited to the simultaneous occurrence of individually extreme drivers. They may also arise when moderate waves, storm surges, tides, or other non-extreme drivers interact and jointly produce severe coastal impacts (Zscheischler et al., 2018). Recent studies have further characterized these interactions as compound coastal hazards and shown that accounting for the dependence among multiple coastal drivers is essential for realistic risk estimation (Zscheischler et al., 2018; Bevacqua et al., 2019; Moftakhari et al., 2017). Therefore, the potential for the simultaneous occurrence of extreme waves and surges is usually considered when designing coastal protection structures, such as seawalls and dikes (SPM, 1984; Goda, 2000; Van der Meer, 1998). However, these extreme phenomena do not always occur simultaneously (Hawkes et al., 2002).

In the Northwest Pacific, typhoons cause the greatest threat to safety of coastal structures and populations. High waves generated by their strong winds and rising storm surges as a result of the low pressure in the typhoon center force the total water level to reach the upper limit of the designed height of sea defenses, thus increasing the associated risks. To illustrate the time lag between maximum wave height and maximum surge during typhoons, this analysis first presents an example with a short time lag and statistical results from Hualien station. Fig. 1 shows the measured significant wave heights, water levels, and storm surges in Typhoon Krosa in 2007 at Hualien station, Taiwan. Notably, the maximum wave height and the highest water level did not occur simultaneously with a small time lag observed. More evidence with the probability distribution is presented in Fig. 2, which illustrates that there exist time lags between the maximum wave height and the highest water level in typhoon events. Although the distribution of time lags is mainly within 6 hours, a considerable number of events exceed this threshold.

* Corresponding author at: Coastal Ocean Monitoring Center, National Cheng Kung University, 1, University Rd., Tainan 70101, Taiwan.
E-mail address: yuchen.ncku@gmail.com (Y.-C. Lee).

https://doi.org/10.1016/j.seares.2026.102736
Received 25 April 2026; Received in revised form 30 August 2026; Accepted 3 September 2026
Available online 8 September 2026
1385-1101/© 2026 The Authors. Published by Elsevier B.V. This is an open access article under the CC BY-NC license (http://creativecommons.org/licenses/by-nc/4.0/).

This indicates that coastal infrastructure design cannot rely on the coincidence of wave and surge peaks. Instead, characterizing their joint probability distribution is necessary for engineering design.

The joint probability of waves and water levels have been applied to coastal defense design and assessment since the 1990s (HR Wallingford and Lancaster University, 2000). This approach was validated by Bruun and Tawn (1998), who demonstrated that multivariate joint probability methods are more accurate than the conventional univariate structure variable approach at multiple Dutch coastlines. Subsequently, Hawkes et al. (2002) developed the joint density approach (JDA), which characterizes the correlation between wave height and water level using bivariate normal distributions combined with Monte Carlo simulation to estimate joint exceedance probabilities. Li and Song (2006) fitted extreme wave heights and surges simulated through a third-generation wave model and a 3D flow model by using generalized extreme value (GEV) distributions and a bivariate logistic model. Studies of the probability distribution of extreme wave heights have revealed that the Weibull distribution describes the distribution of annual maximum wave heights (Forristall, 1978; Mathiesen et al., 1994), and some studies have noted that GEVs represent an improved approach for modeling extreme values (Corbella and Stretch, 2012; Ferreira and Guedes Soares, 2000; Muir and El-Shaarawi, 1986). For extreme wave heights sampled by Peaks-over-threshold (POT), GPDs have been suggested (Guedes Soares and Scotto, 2001; Li et al., 2014; Mazas and Hamm, 2011). Mazas and Hamm (2017) subsequently developed an event-based framework for the joint extremes of waves and sea levels. Moreover, Muir and El-Shaarawi (1986) stated that a compound distribution is more appropriate for data sampled using methods other than annual maxima (AM) (see also Liu et al., 2002; Liu and Ma, 1980). Alternative distributions such as lognormal and gamma distributions have also been proposed for wave height analysis (Dong et al., 2013; Feng et al., 2014; Solari and Losada, 2012). Similar studies have also analyzed water levels, and the results showed that the water level data can be fitted with GEVs (Corbella and Stretch, 2012; Tsimplis and Blackman, 1997). Hawkes et al. (2002) used GPD to model threshold exceedances in the upper tails of wave height and still-water level. Huang et al. (2008) examined the use of GEV for evaluating annual maximum water levels around the

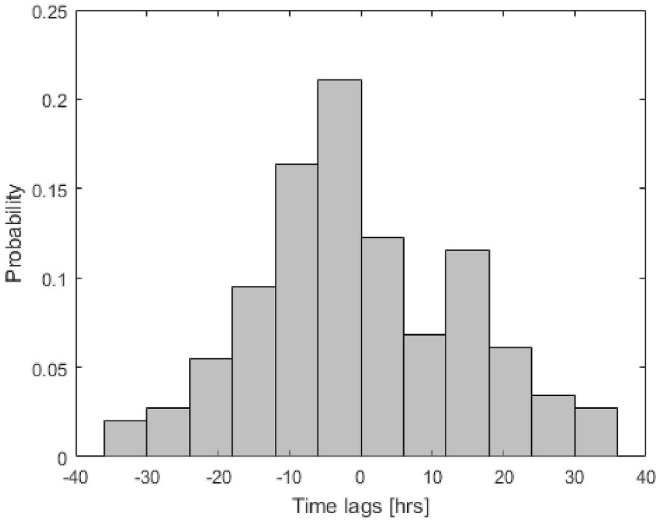


Fig. 2. Distributions of time lags between maxima wave height and maxima surge in typhoon periods (time of maximum wave height − Time of maximum surge). Data were measured at the Hualien station from 2004 to 2014 from 206 typhoons.

United States. Chen and Liu (2016) also applied GEV for the frequency analysis of the maximum surge heights of typhoon events in southwestern Taiwan. In this study, four univariate distributions were selected for fitting the marginal distribution of wave heights and storm surges: three-parameter gamma distribution (GM3), three-parameter lognormal distribution (LN3), GEV, and GPD.

While these traditional bivariate approaches provided valuable insights into dependence, they are often limited by restrictive assumptions on linearity and distributional form (Janse et al., 2021). Therefore, copula-based methods emerged subsequently as a more flexible framework for characterizing complex dependence structures. A copula is a multivariate distribution function with uniform marginal distributions that links univariate marginal distributions to their joint distribution

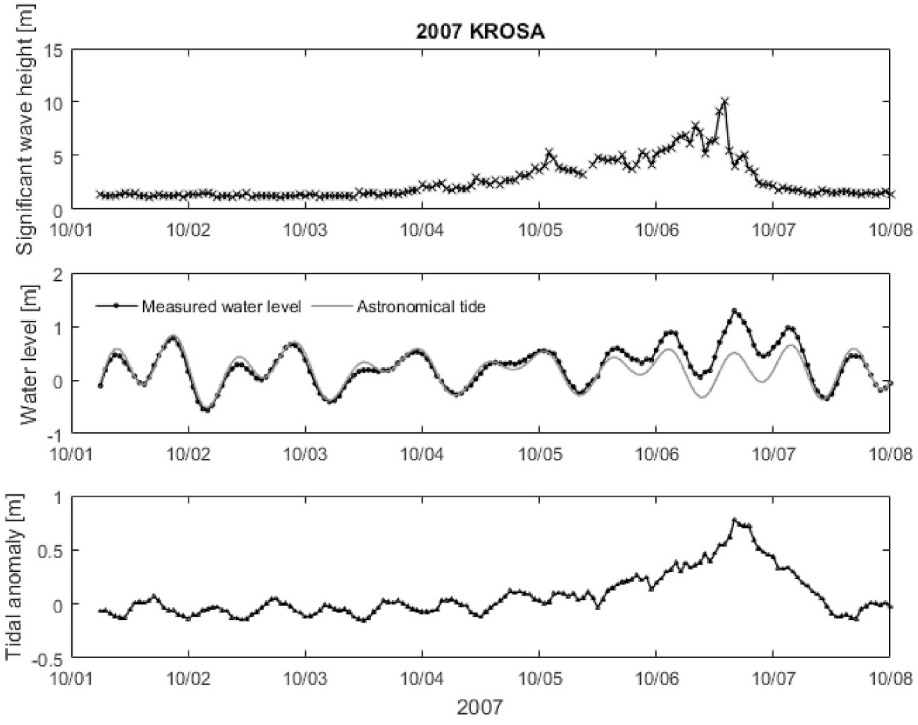


Fig. 1. Time series of wave height, water level, and storm surge (tidal anomaly) during Typhoon Krosa in 2007. Data were measured at the Hualien buoy station.

and characterizes the dependence structure among variables. The advantage of this approach is that univariate marginal distributions are separated without restriction by using the dependence model represented by a copula, which describes the correlation between random variables (Nelsen, 2006; Rüschendorf, 2013). The application of copulas has expanded from hydrology (Salvadori and De Michele, 2004; Volpi and Fiori, 2014) to offshore and coastal engineering (De Michele et al., 2007; Li et al., 2014; Salvadori et al., 2014). They are now extensively used to model the joint probability of various metocean variables, including combinations of wave height, wave period, storm duration, and water levels (e.g., de Waal and van Gelder, 2005; Tao et al., 2013), as well as to investigate coastal erosion (Corbella and Stretch, 2012; Li et al., 2013) and flooding (Masina et al., 2015; Jalili Pirani and Najafi, 2022; Zhu et al., 2024). Alongside these data-driven multivariate approaches, process-based probabilistic hazard frameworks have also evolved. The Joint Probability Method with Optimal Sampling (JPM-OS) selects a limited set of synthetic tropical cyclones that efficiently spans the storm-parameter space, thereby reducing the number of direct wind–wave–surge simulations required (Resio, 2007; Toro et al., 2010; Nadal-Caraballo et al., 2015). More recently, the Joint Probability Method Aided by Metamodel Prediction (JPM-AMP) has used metamodel predictions to augment the storm-response space and further reduce reliance on computationally expensive hydrodynamic simulations (Nadal-Caraballo et al., 2024).

Traditionally, the typhoon intensity classifications used for early warning systems rely primarily on meteorological parameters, such as maximum sustained wind speed and central pressure. This study estimates the joint probability distribution of extreme wave heights and storm surges using a copula-based analysis of typhoon field data. By doing so, we offer a station-based, observation-driven approach to enhance local hazard classification. However, current official typhoon warning systems, which rely primarily on meteorological parameters such as maximum wind speed or central pressure, often fail to adequately reflect the potential for coastal inundation and structural damage caused by compound wave-surge events. The proposed framework may provide information for site-specific coastal hazard assessment where local wave and storm-surge observations or forecasts are available.

This paper is structured as follows. The methodology, including marginal distributions, copula functions, and the Poisson bivariate compound extreme value distribution, is detailed in Section 2. The data collection process is described in Section 3. The results of the analysis, starting with the redefined typhoon influence periods which significantly affect the outcomes, are presented in Section 4.1, followed by the joint probability analysis in Section 4.2. Finally, the proposed typhoon intensity scale based on these joint probabilities is discussed, and the study's conclusions are summarized in Section 5.

2. Methodology

2.1. Marginal distributions

Numerous univariate probability distributions are used to describe the extreme values of variables. The distributions used in this study are presented in Table 1. Fisher and Tippett (1928) proposed the Fisher–Tippett distribution (also known as GEV), which is a noteworthy contribution to the relevant literature, for independent and identical distributed maximum data (normally AM). By the extreme value theorem, only three limiting distributions exist: extreme value distribution types I, II, and III. Prominent distributions, such as the Weibull distribution, are special instances of GEVs, while the Rayleigh distribution is a special case of the Weibull family. The GEV probability density function is characterized by a shape parameter (κ), a location parameter (μ), and a scale parameter (σ). The three aforementioned types of GEV are also called the Gumbel, Fréchet, and reverse Weibull distributions, respectively. When the shape parameter equals zero ($\kappa = 0$), GEV reduces to type I (Gumbel distribution). For positive shape parameters ($\kappa > 0$), GEV corresponds to type II (Fréchet distribution), while for negative shape parameters ($\kappa < 0$), it corresponds to type III (reverse Weibull distribution).

Table 1
Univariate distribution functions used in this study.

Name of distribution	Probability density function
Generalized Extreme Value Distribution (GEV)	$f(x) = \begin{cases} \frac{1}{\sigma}\exp\left(-(1+\kappa z)^{-\frac{1}{\kappa}}\right)(1+\kappa z)^{-1-\frac{1}{\kappa}} \text{ for } \kappa \neq 0, \sigma > 0 \\ \frac{1}{\sigma}\exp(-z-\exp(-z)) \text{ for } \kappa = 0, \sigma > 0 \end{cases}$ where $z \equiv (x-\mu)/\sigma$
Generalized Pareto distribution (GPD)	$f(x) = \begin{cases} \frac{1}{\sigma}\left(1+\kappa\frac{(x-\mu)}{\sigma}\right)^{-1-1/\kappa} \text{ for } \kappa \neq 0, \sigma > 0 \\ \frac{1}{\sigma}exp\left(-\frac{(x-\mu)}{\sigma}\right) \text{ for } \kappa = 0, \sigma > 0 \end{cases}$
Three parameters Gamma Distribution (GM3)	$f(x) = \frac{(x-\mu)^{\kappa-1}}{\sigma^{\kappa}\Gamma(\kappa)}\exp(-(x-\mu)/\sigma)$ for $\kappa > 0, \sigma > 0$
Three parameters Lognormal Distribution (LN3)	$f(x) = \frac{1}{\sqrt{2\pi}\sigma(x-\mu)}\exp\left(-\frac{(\ln(x-\mu)-\kappa)^2}{2\sigma^2}\right)$ for $x > \mu \geq 0, -\infty < \kappa < \infty, \sigma > 0$

GPD has been recommended because of the increased use of the POT method, which has been believed to be a more effective data sampling method than the AM method (Wang, 1991). The GPD includes both exponential ($\kappa = 0$) and Pareto distributions ($\kappa > 0$) as special limiting cases. In the estimation of the upper tail of probability distributions, the GPD-based POT model under the assumption of Poisson-distributed threshold exceedances is asymptotically equivalent to the GEV distribution for block maxima with the same shape parameters in both frameworks (Smith, 1989; Coles, 2001).

The three-parameter gamma distribution (GM3), known as the Pearson type III distribution, is frequently used in hydrologic frequency analyses due to its flexibility in modeling asymmetric distributions (Durrans, 1992). Special cases of the GM3 distribution include chi-square and exponential distributions (Forbes et al., 2011). The three-parameter lognormal (LN3) provides another flexible framework for fitting non-negative environmental data, approaching a normal distribution as κ becomes small (Limpert et al., 2001).

To assess which the selected data follows the best abovementioned distribution, we first estimate the optimal distribution parameters using maximum likelihood estimation (Myung, 2003). Subsequently, we apply Kolmogorov–Smirnov (K—S) goodness-of-fit testing to assess agreement between empirical and theoretical cumulative distribution functions (Massey Jr, 1951). Since parameters are estimated from the data themselves, we employ Monte Carlo simulation with multiple replicates to obtain corrected p-values that account for this estimation bias, thereby ensuring robust statistical validation of distributional assumptions (Robert et al., 1999).

2.2. Copula functions

According to Sklar's theorem (Sklar, 1959), the joint cumulative distribution function (CDF) of two continuous random variables, X and Y, denoted as $G(x,y)$, can be expressed in terms of their marginal CDFs and a copula function. Let $G_X(x)$ and $G_Y(y)$ denote the marginal CDFs of X and Y, respectively. The joint CDF can then be written as:

$$G(x,y) = Pr[X \leq x, Y \leq y] = C(G_X(x), G_Y(y)) = C(u,v), \quad (1)$$

where $u = G_X(x)$ and $v = G_Y(y)$ are probability integral transformed variables that are uniformly distributed on [0,1]. The function C(u, v) is a bivariate copula, namely a distribution function defined on $[0,1]^2$ with uniform marginal distributions.

Copulas characterize the dependence structure between variates through dependence parameters. These parameters can be transformed to other rank-based dependence measures, such as Kendall's τ_K or Spearman's ρ_s. Common copulas used in hydrology and coastal engineering include elliptical and Archimedean families (Salvadori et al., 2007). In this study, the Gaussian, GH, Clayton, and Frank copulas were selected to represent contrasting dependence structures. The GH copula allows upper-tail dependence, which is relevant to the joint occurrence of large wave heights and storm surges. The Clayton copula represents lower-tail dependence, whereas the Gaussian and Frank copulas provide symmetric, tail-independent alternatives.

The elliptical copula family is used for bivariate distributions where both marginal distributions are assumed to be elliptically distributed (Salvadori et al., 2007). The elliptical copula family includes the Gaussian copula (also called the Normal copula), which is the copula of BVN and allows equal degrees of positive and negative dependence. The Gaussian copula can be represented as Eq. (2) for its CDF and Eq. (3) for the PDF.

$$C(u,v) = \int_{-\infty}^{\phi^{-1}(u)} \int_{-\infty}^{\phi^{-1}(v)} \frac{1}{2\pi\sqrt{1-\theta^2}} \exp\left(\frac{x^2 - 2\theta xy + y^2}{2(1-\theta^2)}\right) dxdy \tag{2}$$

$$c(u,v) = \frac{1}{\sqrt{1-\theta^2}} \exp\left\{\frac{x^2+y^2-2\theta xy}{2(1-\theta^2)}\right\} \exp\left\{\frac{x^2+y^2}{2}\right\} \tag{3}$$

where $\theta \in [-1,1]$ is the linear dependent parameter, and ϕ^{-1} denotes the inverse of univariate Normal distribution.

Archimedean copula families include the GH copula, Clayton copula, and Frank copula. Both the GH copula and Clayton copula only allow positive dependence between the margins, whereas the Frank copula allows both positive and negative dependence. The bivariate GH copula is used in the following form:

$$C(u,v) = exp\left\{-\left[(-lnu)^\theta + (-lnv)^\theta\right]^{1/\theta}\right\} \tag{4}$$

$$c(u,v) = \frac{C(u,v)(lnu^* lnv)^{\theta-1}}{uv\left[(-lnu)^\theta + (-lnv)^\theta\right]^{2-1/\theta}} \left\{\left[(-lnu)^\theta + (-lnv)^\theta\right]^{1/\theta} + \theta - 1\right\} \tag{5}$$

where $C(u,v)$ and $c(u,v)$ are the CDF and PDF of GH copula, respectively. The dependence parameter θ spans the interval of $[1,\infty]$, and its relationship to Kendall's τ_K is $\tau_K = 1 - \theta^{-1}$. The uniform random variables are independent when θ approaches 1. The GH copula is suitable for describing data with strong correlation at high values and weakly correlated data at low values.

In contrast to the GH copula, the Clayton copula exhibits strong left tail dependence and weak right tail dependence. It is expressed as

$$C(u,v) = \left(u^{-\theta} + v^{-\theta} - 1\right)^{-\frac{1}{\theta}} \tag{6}$$

$$c(u,v) = (\theta+1)\left(u^{-\theta} + v^{-\theta} - 1\right)^{-\frac{1}{\theta}-2} (uv)^{-\theta-1} \tag{7}$$

where θ is restricted to the interval of $(0,\infty)$ and gives Kendall's τ_K with relationship of $\tau_K = \theta/(\theta+2)$. The margins are independent when $\theta = 0$.

Differing from the GH and Clayton copulas, which model asymmetric dependence in the data, the Frank copula is used to model symmetric dependence (similar to the Gaussian copula). However, the Frank copula has stronger dependence in the middle of the distribution and relatively weak tail dependence; it is also popular because it allows all real values of dependence parameters. The CDF and PDF of the Frank copula can be written as

$$C(u,v) = -\frac{1}{\theta}\ln\left[1 + \frac{(e^{-\theta u}-1)(e^{-\theta v}-1)}{(e^{-\theta}-1)}\right] \tag{8}$$

$$c(u,v) = \frac{\theta\eta e^{-\theta(u+v)}}{[\eta - (1-e^{-\theta u})(1-e^{-\theta v})]^2} \tag{9}$$

here $\theta \in (-\infty,\infty)$, $\eta = 1 - e^{-\theta}$. The Kendall rank can be obtained using $\tau_K = 1 + 4[D_1(-\theta) - 1]/\theta$, and D_1 is the Debye functions of order one.

The copula parameters are estimated using the maximum likelihood method, and the model selection is conducted using the Akaike information criterion (AIC) (Akaike, 1974; Burnham and Anderson, 2002; Claeskens and Hjort, 2008). In this study, AIC is utilized strictly to determine the preferred copula among the candidate families (Fermanian, 2005). Zhang and Singh (2007) further developed AIC with mean square error (MSE) of the fitting and defined it as:

$$AIC = Nln(MSE) + 2k \tag{10}$$

$$MSE = \frac{1}{N}\sum_{i=1}^{N}[p_c(i) - p_0(i)]^2 \tag{11}$$

where N is the number of data points (i.e., sample size), k is the number of free parameters in the model (two for the bivariate copula), MSE is the mean square error, and $p_c(i)$ and $p_0(i)$ are the ith measured and estimated probabilities, respectively. The copula with the lowest AIC is selected as the optimal model.

Once the optimal copula is selected, the joint cumulative distribution function (CDF) is obtained from Eq. (1), and the corresponding joint probability density function (PDF) is expressed as:

$$g(x,y) = c(G_X(x), G_Y(y)) \bullet g_X(x) \bullet g_Y(y) \tag{12}$$

where $c(G_X(x), G_Y(y))$ is the copula density function, and $g_X(x)$ and $g_Y(y)$ are the PDFs of the marginal distributions.

2.3. Poisson bivariate compound extreme value distribution

The compound extreme value distribution (CEVD) is a probability distribution formulated to capture the stochastic behavior of extreme event occurrence in extreme value frequency analysis. The number of occurrences of these events is typically modeled using a discrete distribution, with the Poisson distribution being one of the most frequently used (Liu et al., 2002). For data sets sampled by POT, the compound distribution fits the data more appropriately than conventional univariate approaches (Muir and El-Shaarawi, 1986). CEVD does not restrict the type of marginal distribution or the joint distribution for multivariate CEVD. This method has been widely applied to extreme wind speed prediction (Liu and Ma, 1980), flood frequency analysis (Kirby and Moss, 1987), and storm surge analysis (Tao et al., 2013). After comparing CEVD with six conventional distributions, Muir and El-Shaarawi (1986) concluded that CEVD had a better fit with their wave height data.

The concept of the compound distribution was proposed by Feller (1957). The compound distribution includes the effect of the data sampling method by adding the discrete distribution, which represents extreme events, if the number of sampled data has a specific distribution (p_k):

$$F_0(x) = \sum_{k=0}^{\infty} p_k[G(x)]^k \tag{13}$$

where $F_0(x)$ is the univariate CEVD, $G(x)$ is distribution function of sampled data X, which can be the continuous distribution of any type, and k is the number of events that occur.

Liu et al. (2002) extended the univariate CEVD in Eq. (13) into two dimensions by expressing it as

$$F_0(x,y) = p_0 + \sum_{k=1}^{\infty} p_k \bullet k \bullet \int_{-\infty}^{y}\int_{-\infty}^{x} G_x(u)^{k-1} g(u,v)dudv \tag{14}$$

where $F_0(x,y)$ is bivariate CEVD, p_0 is the probability of a nonevent, and $G_x(u)$ and $g(u,v)$ are the marginal distributions of X and joint PDF, respectively.

The extreme event mentioned above is typhoon for this study. The number of occurrences of typhoons has been found to follow the Poisson distribution (Haring and Heideman, 1978; Liu et al., 2006; Salvadori et al., 2007). Considering n as the annual number of statistically independent typhoon-induced coastal hazard events per year, the occurrence probability can be presented as

$$P\{n=k\} = P_k = \frac{e^{-\lambda}\lambda^k}{k!}, k = 0,1,2\ldots \tag{15}$$

where k is a possible realized number of events (i.e., the number of typhoons per year), and λ is the mean annual occurrence rate of independent events, estimated as the total number of typhoon-induced events divided by the number of observation years.

Substituting Eq. (15) into Eq. (14), and noting that the bivariate continuous distribution can be any type of distribution that fits the data, Eq. (14) can be reformulated as

$$\begin{aligned} F_0(x,y) &= e^{-\lambda} + \sum_{k=1}^{\infty}\int_{-\infty}^{y}\int_{-\infty}^{x}\frac{e^{-\lambda}\lambda^k}{k!}k[G_x(u)]^{k-1}g(u,v)dudv \\ &= e^{-\lambda}\left(1+\lambda\int_{-\infty}^{y}\int_{-\infty}^{x} e^{\lambda G_x(u)}g(u,v)dudv\right) \end{aligned} \tag{16}$$

where (X, Y) is defined as

$$(X,Y) = \begin{cases} (\zeta,\gamma), & n=0 \\ (\xi_j,\eta_j), & \xi_j = \max_{1\le i\le n}\xi_i, n\ge 1 \end{cases} \tag{17}$$

where n is the number of typhoons per year, (ζ,γ) and (ξ,η) represent two continuous random vectors for $n=0$ (no typhoon years) and $n\ge 1$ (typhoon years) cases, respectively.

In this study, (ξ,η) are the typhoon-induced wave heights and their associated storm surge heights in typhoon years, and (ζ,γ) indicates non-typhoon years. $G_x(u)$ is obtained from results of univariate distribution analysis and $g(u,v)$ from results of copula fitting (Eq. (12)).

2.4. Return period analysis of compound wave–surge events

For block maxima (AM) data, the joint return period is typically defined as the inverse of the joint exceedance probability:

$$T(x,y) = \frac{1}{Pr[X>x, Y>y]} \tag{18}$$

Our study is based on AND approach represents the average time between events where both variables simultaneously exceed their thresholds. However, alternative definitions exist including the OR approach and conditional formulations, which are suited to different risk scenarios (Salvadori and De Michele, 2004; Salvadori et al., 2016). The joint return periods are longer for AND case because it requires all variables to exceed their thresholds simultaneously (Khajehali et al., 2025). We use AND definition our coastal hazard application, as significant risk strictly requires the coincident occurrence of these two extreme variables. However, the present study does not use a conventional AM sample. Instead, an event-based typhoon maxima approach is adopted, in which each independent typhoon influence period contributes one maximum significant wave height and storm surge.

For POT data with multiple extreme events per year, it is necessary to estimate the average number of events per year (Khaliq et al., 2006). The joint return period $T(x,y)$ can be regarded as the average duration between two maxima in successive events. The rate parameter λ, which is the average annual rate of statistically independent typhoon events at the study location, is used to correct the aforementioned formula (Lang et al., 1999; Salvadori and De Michele, 2004). The return period becomes

$$T(x,y) = \frac{1}{\lambda\, Pr[X>x, Y>y]} \tag{19}$$

When employing a copula-based approach, the joint return period can be expressed in terms of the copula function and the marginal distributions (Salvadori and De Michele, 2004):

$$T(x,y) = \frac{1}{\lambda\,[1 + C(G_X(x), G_Y(y)) - G_X(x) - G_Y(y)]} \tag{20}$$

where C is the copula function, and G_X are G_Y are the marginal CDFs of wave height and surge.

3. Data collection

For marine meteorology forecasting and designing coastal protection, numerous data buoys and tidal stations have been installed in and around water bodies in Taiwan. The data of wave buoy and tide observations were provided by the Central Weather Bureau (CWB), Taiwan, and the deployment, operation, and maintenance of the monitoring network are conducted by the Coastal Ocean Monitoring Center (COMC), National Cheng Kung University (NCKU), Taiwan (Doong et al., 2007; Doong et al., 2011; Lee et al., 2024). Data buoys are automated meteo-oceanographic platforms that continuously record in situ atmospheric and oceanic conditions. Each buoy has a diameter of 2.5 m and measures wind speed and direction, air and water temperature, air pressure, wave height, wave period, and wave spectra. Wave variables are recorded using a three-dimensional accelerometer with a sampling rate of 2 Hz and are processed into hourly records at the beginning of each hour. Tidal stations are normally installed at harbors. Ultrasonic tidal gauges continuously measure tidal levels every second, and average tidal levels are recorded on an hourly basis. The storm surge data used here were obtained directly as tidal residuals from the CWB, where the astronomical tide was already separated using standard harmonic analysis. The instruments are calibrated and maintained regularly, and the data are well controlled with rigorous checking procedures to ensure reliable quality (Doong et al., 2007).

This study analyzes data from two coastal sites in Taiwan: Longdong in the northeast and Hualien in the east. The data span from 2001 to 2014 for Longdong and from 2004 to 2014 for Hualien. The locations of the wave buoy and tidal station are shown in Table 2. Longdong and Hualien were selected because they are located on the typhoon-exposed northeastern and eastern coasts of Taiwan, respectively, and provide relatively long-term wave and tidal observations. These stations therefore represent local coastal environments and are applicable to surrounding regions with similar environmental conditions. For other areas, the same procedure can be adopted to develop compound wave–surge hazard assessments when field observations are available.

A typhoon is a tropical cyclone characterized by organized deep convection and sustained maximum surface winds that occurs in the Northwest Pacific Ocean basin. On average, 26.8 typhoons occur

Table 2
Information on the locations and data used in this study.

Study site	Wave buoy		Tidal gauge	Measurement duration
	Location	Water depth	Location	
Longdong	25.10° N 121.92° E	30 m	25.16° N 121.75° E	2001-2014
Hualien	24.04° N 121.63° E	21 m	23.97° N 121.62° E	2004-2014

annually in the western North Pacific Ocean (Liu and Chan, 2013), with approximately 4.5 affecting Taiwan (Lee et al., 2006). The CWB of Taiwan issues sea and land typhoon warnings as its official early warning system. A sea typhoon warning is issued when gale-force winds of Beaufort scale ≥7 are forecast to affect marine areas within 100 km of Taiwan within 24 h, alerting maritime, fisheries, and offshore sectors. A land typhoon warning is issued when similar wind conditions threaten terrestrial areas within 18 h. In practice, land typhoon warnings are generally issued after sea typhoon warnings. Based on historical records from 2001 to 2017, the average duration of typhoon warnings issued by the CWB is approximately 54.6 h. Previous studies have used the official warning duration to define the typhoon period for analysis (Chen et al., 2018; Huang and Wang, 2015; Lin et al., 2009).

4. Results and discussion

4.1. Redefined typhoon influence periods

Official typhoon warnings from CWB are issued based on meteorological threat assessment for broad geographic areas. Consequently, they do not accurately reflect local coastal effects. Many regions experience calm sea conditions when warnings are active, leading to inadequate evacuation alerts for coastal residents, fishing operations, and maritime activities. A redefined typhoon influence period based on actual coastal responses is therefore necessary for accurate coastal protection assessment.

This study redefines the typhoon influence period to account for sea-state variables that directly cause coastal damage. Fig. 3 illustrates the three criteria used to identify typhoon influence periods: wave height, swell characteristics, and tidal anomaly. The criteria identify typhoon influence period:

- Wave heights exceeding the 95th percentile of monthly background values (non-typhoon periods).
- The existence of a swell that has a wave height (H_s) larger than 1 m and a wave period (T_p) longer than 11 s.
- Tidal anomaly above a defined threshold set at 0.2 m.

These thresholds were deliberately chosen to reflect actual operational warning practices in Taiwan, based on empirical coastal warning criteria utilized by the COMC, which provides operational guidance to the CWB. The typhoon influence period covers all times when any of these conditions occur. The redefined influence period varies by location due to differing local sea states. It is determined by the above conditions rather than typhoon tracks, so POT sampling is suggested to be generally lower than typhoon counts by their tracks.

Analysis of two Taiwan coastal areas reveals important discrepancies with official warnings. Table 3 compares the number and average duration of selected typhoons as defined by CWB and this study. The average redefined influence period exceeds the official warning duration. Of the 331 and 258 typhoons initially screened for Longdong and Hualien, respectively, 91 and 77 met at least one station-specific influence criterion and were retained. The remaining 240 events at Longdong and 181 events at Hualien were excluded because none of the local criteria was satisfied. It can be seen that compared to the number of typhoons with warnings issued by the official CWB, our proposed criteria yield a slightly higher number of influenced typhoons under the proposed criteria, increasing from 86 to 91 at Longdong for the period 2001–2014 and from 65 to 77 at the Hualien station for 2004–2014. This indicates that the official CWB warnings actually underestimate some periods or events that may cause coastal hazard potential.

One example of an effective typhoon influence period for Typhoon Krosa in 2007 is shown in Fig. 4. The typhoon influence period defined by this study is represented by the gray shaded area, and the current typhoon warning period is represented by the black box. In this figure, the solid, dashed, and dotted lines are time series of wave heights, tidal anomaly, and wave periods, respectively. It can be observed that typhoons caused changes to the coast before they were close enough for warnings to be issued. The redefined typhoon influence period provides more accurate and complete periods to reflect actual typhoon effects for local locations.

4.2. Joint probability analysis

In this study, the joint probabilities of wave heights and storm surges

Table 3
Comparison of typhoon durations.

	Study sites (data period, year)	Longdong (2001-2014)	Hualien (2004-2014)
	Total typhoon number	331	258
Current (general) Typhoon warning	Numbers	86	65
	Average duration (hours)	57.3	55.6
Effective typhoons for the coasts	Numbers	91	77
	Average duration (hours)	87	88

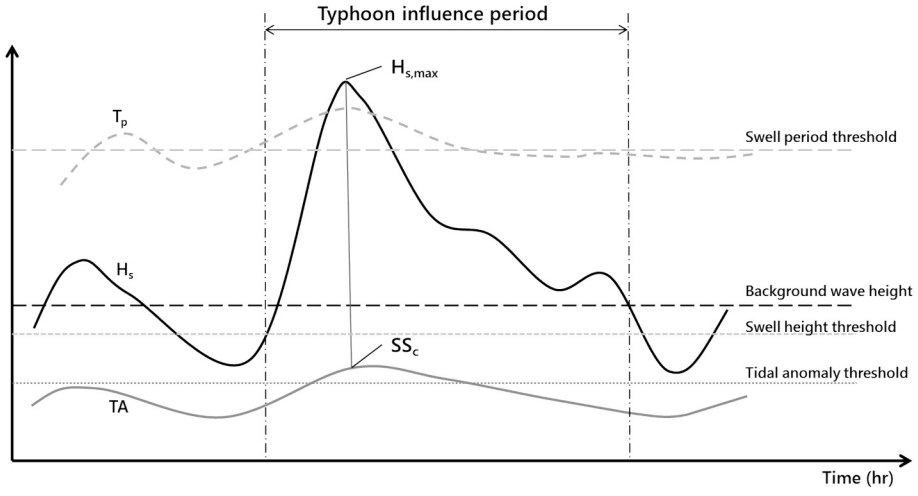


Fig. 3. Sketch of typhoon influence period.

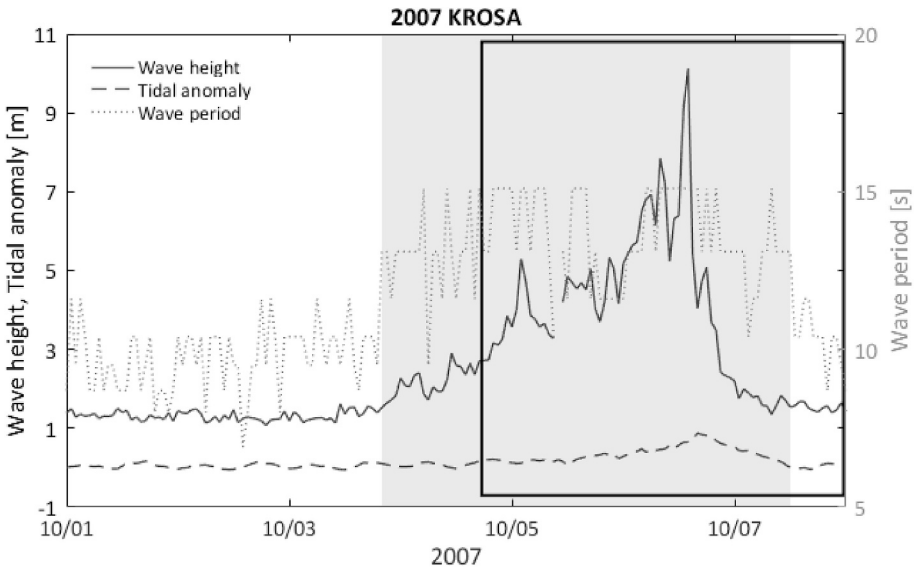


Fig. 4. An example of effective typhoon (Typhoon Krosa in 2007) for Hualien coast. The duration of the typhoon influence time for the coast is represented as a gray shaded area (this study) and black box (current warning period).

at the northeastern coast (Longdong area) and the eastern coast (Hualien area) of Taiwan were analyzed because these areas are the most affected by typhoons. While the Annual Maximum (AM) and Peaks Over Threshold (POT) are commonly used sampling methods in extreme value analysis (Hawkes et al., 2008; Mazas and Hamm, 2017), traditional POT methods require complex declustering and threshold selection criteria (Coles, 2001; Lang et al., 1999). Therefore, since typhoons are the primary drivers of extreme coastal hazards in this region, a 'typhoon-event peak sampling with POT threshold' approach was applied.

Rather than using a conventional constant statistical threshold, the POT threshold in this study is practically defined by the redefined typhoon influence periods. Specifically, a storm event is only considered for sampling if the local sea states exceed at least one of the physical criteria. During the screening process, any meteorological typhoon events that failed to trigger at least one of these local coastal thresholds were excluded from the analysis. For the remaining valid events, the maximum value of each typhoon (i.e., the maximum significant wave height) and its concomitant storm surge was used. To ensure statistical independence and achieve natural declustering, only a single peak value was extracted per discrete typhoon event. If consecutive typhoon influence periods overlapped, they were effectively separated using local wave height minima to ensure each meteorological system was independently represented. However, the historical dataset was limited to approximately 100 events, which is insufficient for robustly estimating high-return-period extremes. To overcome this limitation, Monte Carlo simulation was used to generate a large sample of synthetic events based on the fitted copula model. Because the distribution of each variable and its dependence are essential elements of joint probability of extremes, the simulation was conducted with bivariate copulas derived using the following procedure (Li et al., 2014). The distributions of each variable were first obtained, and the copula of two extremes was fitted based on these marginal distributions. Random samples of two variables were generated from the copula, and the simulated data were then transformed from the random samples of their marginal distributions. Ten thousand samples of each variate were simulated.

The probability distributions of the maximum wave height and storm surge were examined through four common distributions introduced in Section 2.1. Among these distributions, the GEV distribution was selected for the subsequent joint-probability analysis. Table 4 presents the fitted parameters and the goodness-of-fit results, including the K—S and Pearson chi-square statistics and their corresponding *p*-values. The GEV model was not rejected for either variable at Hualien. At Longdong, however, Pearson's chi-square test rejected the fitted GEV models for both variables, and the bootstrap K—S test also rejected the model for storm surge. Therefore, the GEV distributions at Longdong are retained as selected models for the subsequent analysis, but their inadequate goodness of fit may introduce additional uncertainty into the estimated joint probabilities and return levels. The selected distributions are interpreted as the preferred models among the candidates rather than as formally validated fits.

According to the selected marginal distributions listed in Table 4, four types of bivariate copulas were applied to construct the joint distribution $G(x,y)$ of the maximum significant wave height and concomitant storm surge based on Eq. (1). In this study, AIC was utilized strictly as a relative model selection criterion to identify the preferred copula. While formal absolute goodness-of-fit testing was not applied, visual inspection of the joint density contours served as a qualitative complement to the model selection process, allowing us to assess the upper tail dependence. The AIC values calculated for Gaussian, Frank, Gumbel, and Clayton copulas showed no significant differences, with approximate values of −350 at Longdong and − 250 at Hualien station. The final copula selection also considered the physical relevance of the dependence structure, particularly upper-tail dependence, thus selecting the

Table 4
Selected GEV marginal distributions and goodness-of-fit results for significant wave heights and storm surges at Longdong and Hualien.

Variable	Location	Distribution	K-S	K-S *p*-value	χ^2	χ^2 p-value	κ: shape parameter	σ: scale parameter	μ: location parameter
Significant wave height	Longdong	GEV	0.051	0.6166	16.192	0.0128	0.06	1.42	3.57
	Hualien	GEV	0.058	0.6351	3.649	0.7240	0.20	1.42	2.65
Storm surge	Longdong	GEV	0.120	0.0001	24.654	0.0004	0.09	0.18	0.47
	Hualien	GEV	0.069	0.3465	6.506	0.3689	0.05	0.12	0.38

GH copula which has greater relevance. Based on the estimated dependence parameters of the selected copulas, the joint PDFs of the variables are illustrated in Fig. 5. It further illustrates the fitted GH copulas, with dependence parameters of $\theta = 1.83$ for Longdong and $\theta = 1.44$ for Hualien. The joint probability distribution and its PDF are obtained through Eqs. (1) and (12). While the bivariate copula models the dependence between wave height and storm surge magnitude, it does not account for the stochastic nature of typhoon occurrence frequency. To address this, the Compound Extreme Value Distribution (CEVD) was constructed by integrating the Poisson distribution of typhoon frequency with the copula-based joint probabilities.

The occurrence probabilities of typhoons were fitted with the Poisson distribution; the parameter λ of the Poisson distribution represents the average number of events per year, corresponding to statistically independent events. They were 7.79 and 8.55 for Longdong and Hualien, respectively. The annual occurrence counts showed no significant monotonic trend over the study period, supporting the stationarity assumption of the Poisson model. The distributions of the number of typhoons per year, represented using histograms, were compared with fitted Poisson distributions (solid lines in Fig. 6). Goodness-of-fit for the annual occurrence counts was quantitatively assessed using the Pearson chi-square test and the discrete Kolmogorov–Smirnov (K—S) test with bootstrap resampling. For Hualien station, neither the bootstrap Pearson chi-square test nor the discrete K—S test rejected the Poisson model ($\chi^2 = 11.04, p = 0.315; D = 0.198, p = 0.130$). For Longdong station, while the K—S test did not reject the model ($D = 0.173, p = 0.136$), but the chi-square test rejected it ($\chi^2 = 102.14, \mathrm{p} = 0.0036$). This localized deviation at Longdong is likely attributable to overdispersion caused by specific extreme years in the observational record. Nevertheless, because the K—S test confirms that the overall cumulative distribution aligns reasonably well, and to maintain methodological consistency across stations, the Poisson distribution was retained as a pragmatic and statistically plausible model for both locations. This choice is also supported by Liu et al. (2002), and these fitted distributions were subsequently used to construct the CEVD.

The compound joint probabilities used in Eq. (16) were constructed by integrating known marginal distributions, the correlation between variables via copulas, and the Poisson distribution of the study data. Fig. 7 presents the resulting joint exceedance probability distributions of CEVD in forms of isolines corresponding to return periods (RP) of 5, 10, 20, 50, 100, and 200 years, respectively. The dark crosses are observations, and the gray circles are simulations. Any pairs of [H_s, SS] on the isolines have the same return period (i.e. the occurrence probability). In other words, infinite combinations of wave heights and storm surges can exist for a specified return year.

A comparison of the joint exceedance probability distribution obtained using copula and CEVD approaches indicates that when considering typhoon frequency, the return values of a specific return year will be smaller. This indicates that in terms of the design height, the design values will actually be smaller. In Fig. 8, the differences in the results of various methods (solid lines for CEVD and dashed lines for copula) are represented in the form of joint exceedance probability. The exceedance probability calculated using the JDA is represented as dotted lines. Colors represent the joint return periods of 10, 25, 50, and 100 years. The results indicate that JDA and copula have fair agreement at marginal distributions; however, the CEVD contours appear to be closer to the JDA contours in the upper-tail region based on the graphical comparison.

The determination of potential pairs of wave heights and storm surges is crucial for design purposes. Following the strategies introduced by Salvadori et al. (2014), this study uses the H-conditional design realization (H-c), which selects a "primary" variable from the univariate distribution to immediately determine the corresponding design value of the secondary variate. Here, we calculated the design value pairs by using H-c, marked as solid black squares in Fig. 7. The design value pairs of H-c are listed in Table 5. The return values of storm surges may be underestimated if the joint probability is not considered, and the design height of coastal protection, if obtained through the simplest method (linear summation), may also be underestimated. Therefore, the selection strategy is crucial, and the summation of influencing factors may also lead to the overestimation of hazard and increased construction costs (Liu et al., 2006). For our cases, the influence of synchronous extreme events may be greater than that of extreme events occurring in isolation and may lead to the failure of the design.

4.3. New assessment for typhoon intensity

Current typhoon intensity classification mainly depends on weather conditions such as the central pressure or maximum sustained wind speed of a typhoon. However, the criteria for the classification and the estimation of sustained winds are inconsistent among countries or regions that experience frequent typhoons, such as the United States, Japan, China, Taiwan, and Australia. For example, the United States National Hurricane Center uses the Saffir–Simpson hurricane wind scale (SSHWS) to classify typhoon intensity. The SSHWS categorizes typhoons into five classes: typhoons with wind speeds above 64, 83, 96, 113, and 137 knots are classified as categories I, II, III, IV, and V, respectively. A typhoon with a maximum sustained wind speed greater than or equal to 137 knots is classified as a category V typhoon, whereas such a typhoon is categorized as a "strong typhoon" according to the typhoon intensity

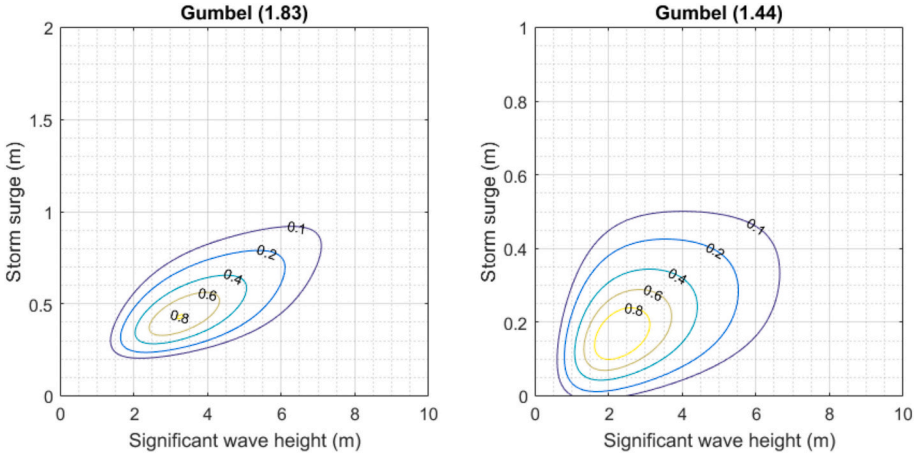


Fig. 5. Joint probability density function of selected copulas for Longdong (left) and Hualien (right).

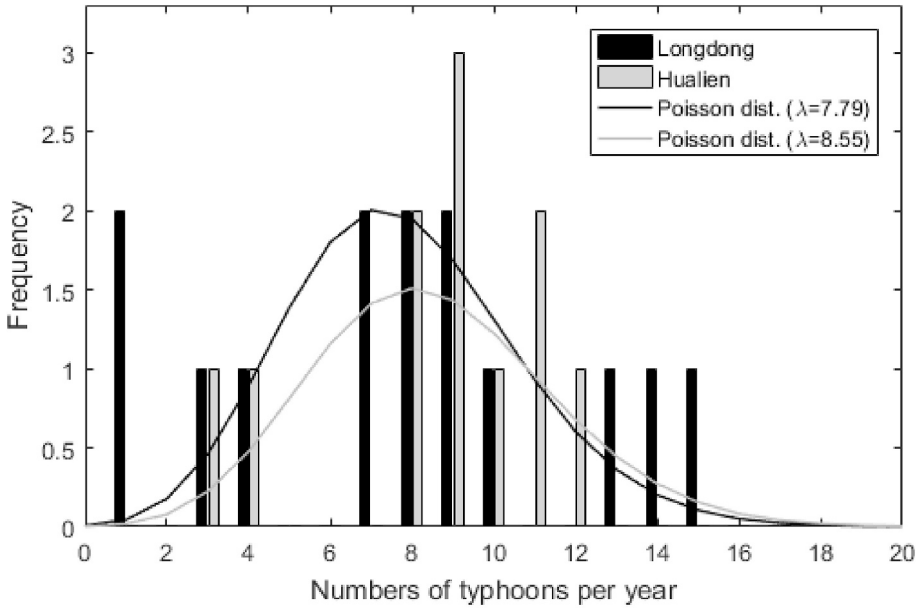


Fig. 6. Annual number of typhoons and the fitted Poisson distribution. The black color represents the Longdong station, and the gray color represents the Hualien station.

scale of the Taiwan CWB, which classifies typhoons into three scales: mild, moderate (equal to SSHWS categories I–III), and strong (equal to SSHWS categories IV–V) typhoons. A high-intensity typhoon exhibits considerable destructive power but may not cause substantial damage because the potential damage is still dependent on the typhoon track, moving speed, weather conditions, and other factors, in addition to typhoon intensity.

The existing typhoon intensity classification methods primarily consider the low pressure or maximum wind speed, but not the potential threat to the coast. Currently, a typhoon that is classified as strong may cause substantial damage to the land because of heavy rainfall or other causes but may not cause coastal damage. The existing typhoon intensity classification is insufficient for providing coastal hazard warnings or assessments. Therefore, in this study, a new typhoon-induced coastal hazard classification was proposed, which can be specifically applied to coastal areas. The new classification method is based on the joint effects of typhoon wave heights and storm surges. Unlike conventional classifications that rely solely on meteorological parameters, the proposed method directly evaluates coastal hazards by integrating wave-surge interactions and their return periods.

In this study, typhoon intensity, which is determined based on typhoon effects, was classified into four scales according to the joint return period. The four scales are as follows: slight impact (SL), moderate impact (MO), severe impact (SE), and destructive impact (DI); typhoons at these scales produce effects with the joint return periods of 0–10, 10–25, 25–50, and more than 50 years, respectively. A total of 91 typhoons that affected the Longdong area were classified based on the typhoon extreme values (Table 6), of which 87 (96%) typhoons were categorized as typhoons with a SL that slightly affected the coast. One typhoon was classified as the MO scale, two typhoons had SE effects, and one typhoon, which caused substantial changes to the coast, was indicated as having DIs. For Hualien area, 73 (95%) typhoons were indicated at the SL scale, 3 of 77 typhoons were indicated at the MO scale, and 1 typhoon was indicated at the DI scale.

To further examine the applicability of the proposed site-specific coastal hazard classification, representative typhoon events were compared with official meteorological classifications and available coastal damage records. Table 7 compares selected typhoon events classified by the CWB and SSHWS, and the proposed site-specific coastal hazard classification. The comparison indicates that meteorological typhoon intensity does not always correspond to local coastal impact. One of the typical cases is Typhoon Soulik in 2013, which caused a maximum wave height of 12.8 m and storm surge of 1.9 m to Longdong; thus, it was categorized as a DI typhoon for Longdong area, whereas a maximum wave height of 4.1 m and storm surge of 0.83 m were observed at Hualien; thus, it was categorized as an SL typhoon for Hualien area.

Available damage records collected from field investigations provide supporting evidence for the proposed classification. During Typhoon Morakot in 2009, the Hualien Harbor breakwater was severely damaged, with an approximately 50 m breach or crack reported along the eastern breakwater. During Typhoon Krosa in 2007, severe coastal erosion was reported along the Hualien coast, including the loss of an approximately 300 m long beach section at Shuilien, while national agricultural and facility losses exceeded NT$4 billion. Typhoon Fanapi in 2010 also caused substantial agricultural losses in Taiwan, with Hualien included among the affected counties and local agricultural losses reported to exceed NT$100 million. Meanwhile, other breakwater damage at the Hualien coast was observed during Typhoon Krosa in 2007 and Fanapi in 2010, indicating MO effects of the typhoons on the coast. However, in some cases, actual damage was not well captured by the proposed index; for example, in the case of Typhoon Haitang in 2005. For moderate threats, such as Typhoon Talim in 2005, no damage records are available. Comparing the CWB scales and SSHWS indicated that the typhoon damage potential to the coast was inconsistent across these scales. For strong typhoons and super typhoons (SSHWS categories IV and V), the coastal effects are not always serious (Table 7). These cases suggest that the proposed classification can provide additional information on local coastal hazard severity that is not directly represented by conventional meteorological classifications.

5. Conclusions

Traditionally, official typhoon intensity classifications and early warning systems rely primarily on meteorological parameters. While these systems are highly effective for broad meteorological forecasting, they are not explicitly designed to capture the localized potential for coastal inundation and structural damage caused by compound wave-surge events. To address this limitation, this paper analyzed the joint effects of extreme wave heights and storm surges by typhoons were

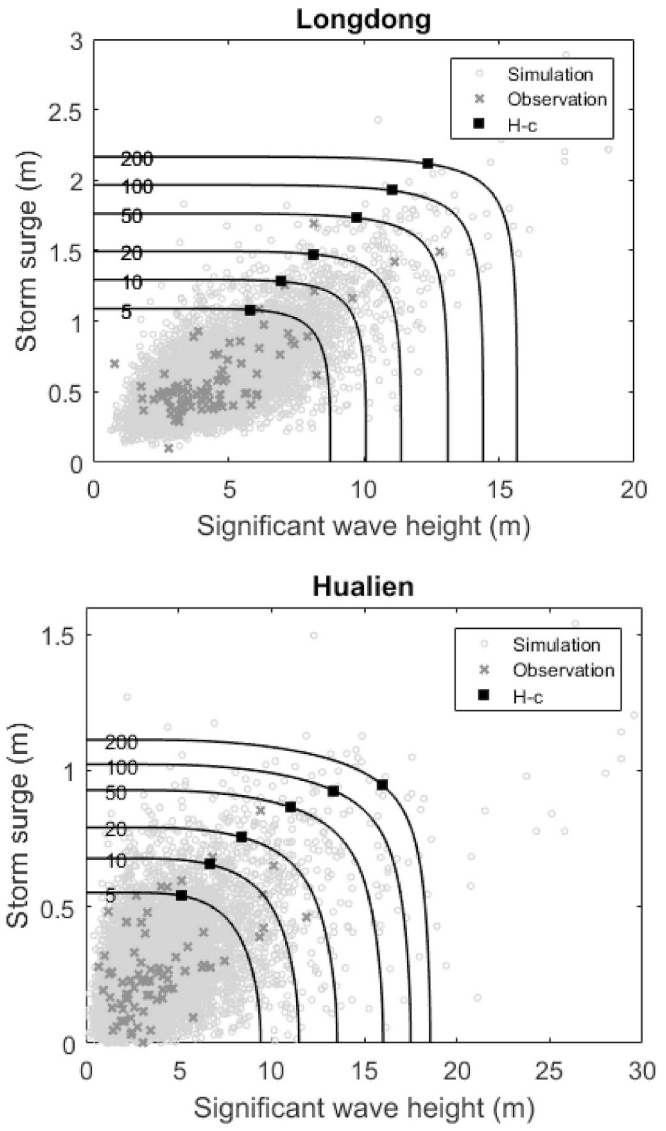


Fig. 7. Joint exceedance probability distribution of significant wave heights and storm surges for return periods of 5, 10, 20, 50, 100, and 200 years (isolines). Dark crosses are observations, light gray circles are simulated data, and solid squares are return value pairs obtained from H-conditional (H-c) design realization.

analyzed using observations collected over approximately 14 years. Typhoon events were selected and their influence periods were redefined based on the criteria of wave height, swell, and storm surge height. A model comprising the marginal distributions of wave heights and storm surges, the correlation between variables, and the frequency of typhoon events was constructed. By conducting simulation, extrapolation, and frequency analysis based on this copula-based model, we offer a station-based approach to enhance local coastal hazard classification.

Four univariate probability distributions were compared to select candidate models for the marginal distribution of typhoon extreme wave heights and storm surges. The generalized extreme value (GEV) distribution was determined to be the optimal model for most cases in this study. Bivariate models were constructed based on four copulas with selected marginal distributions: Gaussian, Gumbel–Hougaard (GH), Frank, and Clayton copulas. The results indicated that the GH copula had comparatively higher performance for the current study data. Moreover, considering the occurrence frequency of typhoons, the Poisson distribution was combined with the bivariate copula function, forming the Compound Extreme Value Distribution (CEVD).

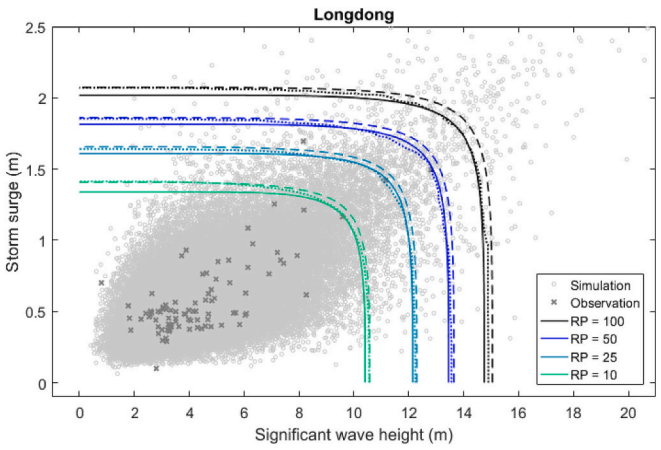


Fig. 8. Comparison of return periods by CEVD (solid lines), copula (dashed lines), and the joint density approach (dotted lines). Colors represent different return periods (RP) in years. The gray circles are simulated data, and the dark crosses are observations.

Table 5
Values of significant wave height (SWH), storm surge (SS), and their summation of certain return periods (years) obtained from H-conditional design realization.

Location	variables	Return period (years)					
		5	10	20	50	100	200
Longdong	SWH (m)	5.80	7.00	8.20	9.80	11.00	12.30
	SS (m)	0.68	0.88	1.08	1.34	1.53	1.72
	Sum (m)	6.48	7.88	9.28	11.14	12.53	14.02
Hualien	SWH (m)	5.10	7.00	8.40	11.00	13.30	16.00
	SS (m)	0.54	0.65	0.75	0.87	0.93	0.95
	Sum (m)	5.64	7.65	9.15	11.87	14.23	16.95

Table 6
Results of the redefined coastal hazard classification for coastal areas.

Classification	Impact for Hualien coast	Impact for Longdong coast
Slight Impact (SL)	73	87
Moderate Impact (MO)	3	1
Severe Impact (SE)	0	2
Destructive Impact (DI)	1	1

Table 7
Intensity of the selected typhoons.

Year	Typhoon name	CWB classification	SSHWS category	This study (for Hualien)	This study (for Longdong)
2013	USAGI	Strong	IV	SL	SL
2013	SOULIK	Strong	IV	SL	DI
2012	JELAWAT	Strong	V	SL	SL
2011	NANMADOL	Strong	V	SL	SL
2011	SONGDA	Strong	V	SL	SL
2008	JANGMI	Strong	V	SL	SE
2008	SINLAKU	Strong	IV	SL	SL
2007	KROSA	Strong	IV	MO	SL
2007	SEPAT	Strong	V	SL	SL
2005	LONGWANG	Strong	IV	SL	SL
2005	TALIM	Strong	IV	MO	SL
2005	HAITANG	Strong	V	SL	SL
2010	FANAPI	Moderate	III	MO	SL
2004	NOCK-TEN	Moderate	III	SL	SE
2013	FITOW	Moderate	II	SL	MO
2009	MORAKOT	Moderate	I	DI	SL

A comparison of the joint exceedance probability between various methods indicated that CEVD appears to be closer to the JDA in the upper-tail region. The design values of the bivariate distribution were obtained using the H-conditional (H-c) design realization and were compared with return values from univariate distributions. The result indicates that the effects of synchronous extreme events are greater, and the summation of the influencing factors lead to an underestimation. Moreover, in this study, a typhoon intensity assessment scale was proposed that considered the typhoon impact to the coast, and this scale was compared with other typhoon intensity scales, which only consider the weather conditions. Damage records verified the new defined categories. Neither CWB typhoon intensity scales nor SSHWS could adequately assess the potential coastal impact, as they are strictly based on meteorological forecasting. Using forecasted data of typhoon wave heights and storm surges, the proposed typhoon-induced coastal hazard classification method can be applied to warn people about potential coastal effects before a typhoon's arrival. This approach provides a more direct assessment of coastal hazards compared to conventional meteorological classifications. Future studies can include more considerations, such as wind speed and direction, to improve the classification and extend to other coastal regions.

While the joint return period estimations in this study rely on a historical observational dataset of over 10 years, climate warming conditions are causing significant changes in typhoon hazard characteristics and tropical cyclone–ocean interaction processes (Guan et al., 2018; Guan et al., 2026). Because the 100- and 200-year return levels carry inherent statistical uncertainties, longer datasets should be used where available. Additionally, since this study is observation-based and station-specific, its spatial applicability remains limited to the selected stations and nearby coasts with similar environmental conditions. Spatially continuous regional hazard estimates and scenario-based assessments can be achieved using coupled wave–surge numerical models such as ADCIRC–SWAN (Jin et al., 2025), though these demand greater computational resources.

CRediT authorship contribution statement

Dong-Jiing Doong: Writing – original draft, Validation, Supervision, Resources, Project administration, Methodology, Investigation, Funding acquisition, Data curation, Conceptualization. **Yu-Chen Lee:** Writing – review & editing, Writing – original draft, Validation, Software, Methodology, Investigation, Formal analysis, Data curation. **Leng-Hsuan Tseng:** Writing – original draft, Visualization, Validation, Software, Resources, Methodology, Investigation, Formal analysis, Data curation, Conceptualization. **Ying-Chih Chen:** Writing – review & editing, Validation, Software, Methodology, Investigation, Formal analysis, Data curation, Conceptualization.

Declaration of competing interest

The authors declare that they have no known competing financial interests or personal relationships that could have appeared to influence the work reported in this paper.

Acknowledgments

The authors thank the anonymous reviewers for their careful review of the manuscript and their numerous insightful and constructive comments and suggestions for improving this paper. This research was supported by the Ministry of Science and Technology of Taiwan (Grant No: MOST 107-3113-E-006-011 and MOST 106-2628-E-006-008-MY3). The buoy data used in this study were measured and qualified by the Coastal Ocean Monitoring Center of National Cheng Kung University. The authors would like to express their gratefulness for all the support.

Data availability

Data will be made available on request.

References

Akaike, H., 1974. A new look at the statistical model identification. IEEE Trans. Autom. Control 19 (6), 716–723.
Bevacqua, E., Maraun, D., Vousdoukas, M.I., Voukouvalas, E., Vrac, M., Mentaschi, L., Widmann, M., 2019. Higher probability of compound flooding from precipitation and storm surge in Europe under anthropogenic climate change. Sci. Adv. 5 (9), eaaw5531.
Bruun, J.T., Tawn, J.A., 1998. Comparison of approaches for estimating the probability of coastal flooding. J. R. Stat. Soc.: Ser. C: Appl. Stat. 47 (3), 405–423.
Burnham, K.P., Anderson, D.R., 2002. Model Selection and Multimodel Inference: A Practical Information-Theoretic Approach. Springer New York, New York, NY.
Chen, W.-B., Liu, W.-C., 2016. Assessment of storm surge inundation and potential hazard maps for the southern coast of Taiwan. Nat. Hazards 82 (1), 591–616.
Chen, C.-J., Lee, T.-Y., Chang, C.-M., Lee, J.-Y., 2018. Assessing typhoon damages to Taiwan in the recent decade: return period analysis and loss prediction. Nat. Hazards 91 (2), 759–783.
Claeskens, G., Hjort, N.L., 2008. Model Selection and Model Averaging. Cambridge Books.
Coastal Engineering Research Center (US), 1984. Shore Protection Manual (SPM), vol. 1. Department of the Army, Waterways Experiment Station, Corps of Engineers, Coastal Engineering Research Center.
Coles, S., 2001. An Introduction to Statistical Modeling of Extreme Values. Springer Series in Statistics, XIV. Springer-Verlag, London, p. 209.
Corbella, S., Stretch, D.D., 2012. Predicting coastal erosion trends using non-stationary statistics and process-based models. Coast. Eng. 70, 40–49.
Cuomo, G., Piscopia, R., Allsop, W., 2011. Evaluation of wave impact loads on caisson breakwaters based on joint probability of impact maxima and rise times. Coast. Eng. 58 (1), 9–27.
De Michele, C., Salvadori, G., Passoni, G., Vezzoli, R., 2007. A multivariate model of sea storms using copulas. Coast. Eng. 54 (10), 734–751.
de Waal, D.J., van Gelder, P.H.A.J.M., 2005. Modelling of extreme wave heights and periods through copulas. Extremes 8 (4), 345–356.
Dong, S., Tao, S., Lei, S., Soares, C.G., 2013. Parameter estimation of the maximum entropy distribution of significant wave height. J. Coast. Res. 288, 597–604.
Doong, D.J., Chen, S.H., Kao, C.C., Lee, B.C., Yeh, S.P., 2007. Data quality check procedures of an operational coastal ocean monitoring network. Ocean Eng. 34 (2), 234–246.
Doong, D.J., Lee, B.C., Kao, C.C., 2011. Wave measurements using GPS velocity signals. Sensors 11 (1), 1043–1058.
Durrans, S.R., 1992. Parameter estimation for the Pearson type 3 distribution using order statistics. J. Hydrol. 133 (3–4), 215–232.
Feller, W., 1957. An Introduction to Probability Theory and its Applications, 2nd ed. vol. 1. John Wiley, Oxford, England, p. 461. xv, 461-xv.
Feng, X., Tsimplis, M.N., Quartly, G.D., Yelland, M.J., 2014. Wave height analysis from 10 years of observations in the norwegian sea. Cont. Shelf Res. 72, 47–56.
Fermanian, J.-D., 2005. Goodness-of-fit tests for copulas. J. Multivar. Anal. 95 (1), 119–152.
Ferreira, J.A., Guedes Soares, C., 2000. Modelling distributions of significant wave height. Coast. Eng. 40 (4), 361–374.
Fisher, R.A., Tippett, L.H.C., 1928. Limiting forms of the frequency distribution of the largest or smallest member of a sample. Math. Proc. Camb. Philos. Soc. 24 (2), 180–190.
Forbes, C., Evans, M., Hastings, N., Peacock, B., 2011. Statistical Distributions. John Wiley & Sons, Inc.
Forristall, G.Z., 1978. On the statistical distribution of wave heights in a storm. J. Geophys. Res. Oceans 83 (C5), 2353–2358.
Goda, Y., 2000. Random seas and design of maritime structures. In: Advanced Series on Ocean Engineering, 15. World Scientific.
Guan, S., Li, S., Hou, Y., Hu, P., Liu, Z., Feng, J., 2018. Increasing threat of landfalling typhoons in the western North Pacific between 1974 and 2013. Int. J. Appl. Earth Obs. Geoinf. 68, 279–286.
Guan, S., Huang, M., Cai, W., Zhang, Z., Lin, I.I., Kim, H.S., Zhou, L., Lin, X., Xu, Z., Jin, F.F., Mei, W., 2026. Weak self-induced cooling of tropical cyclones amid fast sea surface warming. Nat. Geosci. 1–6.
Guedes Soares, C., Scotto, M., 2001. Modelling uncertainty in long-term predictions of significant wave height. Ocean Eng. 28 (3), 329–342.
Haring, R.E., Heideman, J.C., 1978. Gulf of Mexico Rare Wave Return Periods. Offshore Technology Conference.
Hawkes, P.J., Gouldby, B.P., Tawn, J.A., Owen, M.W., 2002. The joint probability of waves and water levels in coastal engineering design. J. Hydraul. Res. 40 (3), 241–251.
Hawkes, P.J., Gonzalez-Marco, D., Sánchez-Arcilla, A., Prinos, P., 2008. Best practice for the estimation of extremes: a review. J. Hydraul. Res. 46 (Sup 2), 324–332.
HR Wallingford and Lancaster University, 2000. The Joint Probability of Waves and Water Levels: JOIN-SEA: A Rigorous but Practical New Approach, HR Wallingford Report SR 537, Originally Dated November 1998, Re-Issued with Minor Amendments in Final Form in May 2000. HR Wallingford, UK.
Huang, W.-K., Wang, J.-J., 2015. Typhoon damage assessment model and analysis in Taiwan. Nat. Hazards 79 (1), 497–510.

Huang, W., Xu, S., Nnaji, S., 2008. Evaluation of gev model for frequency analysis of annual maximum water levels in the coast of United States. Ocean Eng. 35 (11–12), 1132–1147.
Igigabel, M., Yates, M., Vousdoukas, M., Diab, Y., 2023. A systemic and comprehensive assessment of coastal hazard changes: method and application to France and its overseas territories. Nat. Hazards Earth Syst. Sci. Discuss. 2023, 1–35.
Islam, M.F., Bhattacharya, B., Popescu, I., 2019. Flood risk assessment due to cyclone-induced dike breaching in coastal areas of Bangladesh. Nat. Hazards Earth Syst. Sci. 19 (2), 353–368.
Jalili Pirani, F., Najafi, M.R., 2022. Multivariate analysis of compound flood hazard across Canada's Atlantic, Pacific and Great Lakes coastal areas. Earth's. Future 10 (8), e2022EF002655.
Janse, R.J., Hoekstra, T., Jager, K.J., Zoccali, C., Tripepi, G., Dekker, F.W., Van Diepen, M., 2021. Conducting correlation analysis: important limitations and pitfalls. Clin. Kidney J. 14 (11), 2332–2337.
Jin, W., Guan, S., Chen, L., Tang, Z., Huang, M., Xu, X., Zhao, W., 2025. Joint risk analysis of typhoon hazards based on coupled ADCIRC-SWAN model simulations around Hainan, China. J. Sea Res. 205, 102587.
Khajehali, M., Safavi, H.R., Nikoo, M.R., Najafi, M.R., Alizadeh-Sh, R., 2025. A copula-based multivariate flood frequency analysis under climate change effects. Sci. Rep. 15 (1), 146.
Khaliq, M.N., Ouarda, T.B.M.J., Ondo, J.C., Gachon, P., Bobée, B., 2006. Frequency analysis of a sequence of dependent and/or non-stationary hydro-meteorological observations: a review. J. Hydrol. 329 (3–4), 534–552.
Kirby, W.H., Moss, M.E., 1987. Summary of flood-frequency analysis in the United States. J. Hydrol. 96 (1), 5–14.
Lang, M., Ouarda, T.B.M.J., Bobée, B., 1999. Towards operational guidelines for over-threshold modeling. J. Hydrol. 225 (3–4), 103–117.
Lee, C.S., Huang, L.R., Shen, H.S., Wang, S.T., 2006. A climatology model for forecasting typhoon rainfall in Taiwan. Nat. Hazards 37 (1–2), 87–105.
Lee, Y.C., Brühl, M., Doong, D.J., Wahls, S., 2024. Nonlinear Fourier classification of 663 rogue waves measured in the Philippine Sea. PLoS One 19 (5), e0301709.
Li, C.W., Song, Y., 2006. Correlation of extreme waves and water levels using a third-generation wave model and a 3d flow model. Ocean Eng. 33 (5–6), 635–653.
Li, Y., Simmonds, D., Reeve, D., 2008. Quantifying uncertainty in extreme values of design parameters with resampling techniques. Ocean Eng. 35 (10), 1029–1038.
Li, F., et al., 2013. Probabilistic modeling of wave climate and predicting dune erosion. J. Coast. Res. 760–765.
Li, F., van Gelder, P.H.A.J.M., Ranasinghe, R., Callaghan, D.P., Jongejan, R.B., 2014. Probabilistic modelling of extreme storms along the dutch coast. Coast. Eng. 86, 1–13.
Limpert, E., Stahel, W.A., Abbt, M., 2001. Log-normal distributions across the sciences: keys and clues. Bioscience 51 (5), 341–352.
Lin, G.F., Chen, G.R., Huang, P.Y., Chou, Y.C., 2009. Support vector machine-based models for hourly reservoir inflow forecasting during typhoon-warning periods. J. Hydrol. 372 (1–4), 17–29.
Liu, K.S., Chan, J.C.L., 2013. Inactive period of western north pacific tropical cyclone activity in 1998–2011. J. Clim. 26 (8), 2614–2630.
Liu, T.F., Ma, F.S., 1980. Prediction of extreme wave heights and wind velocities. J. Waterway Port Coast. Ocean Div.-ASCE. 106 (4), 469–479.
Liu, D., Wen, S., Wang, L., 2002. Poisson-gumbel mixed compound distribution and its application. Chin. Sci. Bull. 47 (22), 1901–1906.
Liu, D., Wang, L., Pang, L., 2006. Theory of multivariate compound extreme value distribution and its application to extreme sea state prediction. Chin. Sci. Bull. 51 (23), 2926–2930.
Masina, M., Lamberti, A., Archetti, R., 2015. Coastal flooding: a copula based approach for estimating the joint probability of water levels and waves. Coast. Eng. 97, 37–52.
Massey Jr., F.J., 1951. The Kolmogorov-Smirnov test for goodness of fit. J. Am. Stat. Assoc. 46 (253), 68–78.
Mathiesen, M., et al., 1994. Recommended practice for extreme wave analysis. J. Hydraul. Res. 32 (6), 803–814.
Mazas, F., Hamm, L., 2011. A multi-distribution approach to pot methods for determining extreme wave heights. Coast. Eng. 58 (5), 385–394.
Mazas, F., Hamm, L., 2017. An event-based approach for extreme joint probabilities of waves and sea levels. Coast. Eng. 122, 44–59.
Moftakhari, H.R., Salvadori, G., AghaKouchak, A., Sanders, B.F., Matthew, R.A., 2017. Compounding effects of sea level rise and fluvial flooding. Proc. Natl. Acad. Sci. 114 (37), 9785–9790.
Muir, L.R., El-Shaarawi, A.H., 1986. On the calculation of extreme wave heights: a review. Ocean Eng. 13 (1), 93–118.
Myung, I.J., 2003. Tutorial on maximum likelihood estimation. J. Math. Psychol. 47 (1), 90–100.
Nadal-Caraballo, N.C., Melby, J.A., Gonzalez, V.M., Cox, A.T., 2015. Coastal Storm Hazards from Virginia to Maine (No. ERDCCHLTR155).
Nadal-Caraballo, N.C., Yawn, M.C., Aucoin, L.A., Gonzalez, V.M., Carr, M.L., Stehno, A. L., Melby, J.A., Massey, C., Taflanidis, A.A., Bensi, M.T., 2024. Joint probability method aided by metamodel prediction for hurricane hazards. Coast. Eng. Proc. 38, 173.
Nelsen, R.B., 2006. An Introduction to Copulas. Springer Series in Statistics, XIV. Springer-Verlag, New York, p. 272.
Resio, D.T., 2007. White Paper on Estimating Hurricane Inundation Probabilities. US Army Corps of Engineers Engineer Research and Development Center, Vicksburg, MS.
Robert, C.P., Casella, G., Casella, G., 1999. Monte Carlo Statistical Methods, vol. 2. Springer, New York.
Rüschendorf, L., 2013. Mathematical Risk Analysis : Dependence, Risk Bounds, Optimal Allocations and Portfolios. Springer series in operations research and financial engineering, XII. Springer-Verlag, Berlin Heidelberg, p. 408.
Salvadori, G., De Michele, C., 2004. Frequency analysis via copulas: theoretical aspects and applications to hydrological events. Water Resour. Res. 40 (12).
Salvadori, G., De Michele, C., Kottegoda, N.T., Rosso, R., 2007. Extremes in Nature: An Approach Using Copulas. Water Science and Technology Library, XIV. Springer Netherlands, p. 292.
Salvadori, G., Tomasicchio, G.R., D'Alessandro, F., 2014. Practical guidelines for multivariate analysis and design in coastal and off-shore engineering. Coast. Eng. 88, 1–14.
Salvadori, G., Durante, F., De Michele, C., Bernardi, M., Petrella, L., 2016. A multivariate copula-based framework for dealing with hazard scenarios and failure probabilities. Water Resour. Res. 52 (5), 3701–3721.
Sklar, M., 1959. Fonctions de répartition à n dimensions et leurs marges. In: Annales de l'ISUP, Vol. 8, No. 3, pp. 229–231.
Smith, R.L., 1989. Extreme value analysis of environmental time series: an application to trend detection in ground-level ozone. Stat. Sci. 367–377.
Solari, S., Losada, M.Á., 2012. Unified distribution models for met-ocean variables: application to series of significant wave height. Coast. Eng. 68, 67–77.
Tao, S., Dong, S., Wang, N., Guedes Soares, C., 2013. Estimating storm surge intensity with poisson bivariate maximum entropy distributions based on copulas. Nat. Hazards 68 (2), 791–807.
Toro, G.R., Resio, D.T., Divoky, D., Niedoroda, A.W., Reed, C., 2010. Efficient joint-probability methods for hurricane surge frequency analysis. Ocean Eng. 37 (1), 125–134.
Tsimplis, M.N., Blackman, D., 1997. Extreme Sea-level distribution and return periods in the aegean and ionian seas. Estuar Coast Shelf S 44 (1), 79–89.
Van der Meer, J.W., 1998. Geometrical design of coastal structures. In: Pilarczyk, K.W. (Ed.), Dikes and Revetments: Design, Maintenance and Safety Assessment. CRC Press, Rotterdam, Netherlands, pp. 161–177. Iahr hydraulic structures design manuals.
Volpi, E., Fiori, A., 2014. Hydraulic structures subject to bivariate hydrological loads: return period, design, and risk assessment. Water Resour. Res. 50 (2), 885–897.
Wang, Q.J., 1991. The pot model described by the generalized pareto distribution with poisson arrival rate. J. Hydrol. 129 (1), 263–280.
Zhang, L., Singh, V.P., 2007. Bivariate rainfall frequency distributions using archimedean copulas. J. Hydrol. 332 (1–2), 93–109.
Zhu, Z., Zhang, W., Zhu, W., 2024. Compound impact of storm surge and flood characteristics in coastal area based on copula. Water 16 (2), 270.
Zscheischler, J., Westra, S., Van Den Hurk, B.J., Seneviratne, S.I., Ward, P.J., Pitman, A., AghaKouchak, A., Bresch, D.N., Leonard, M., Wahl, T., Zhang, X., 2018. Future climate risk from compound events. Nat. Clim. Chang. 8 (6), 469–477.